

FREE VIBRATION CHARACTERISTICS ON A SPLIT TORQUE TRANSMISSION

¹ZHAOXIA HE, ²LEHAO CHANG, ²LAN LIU

¹Key Laboratory of Road Construction Technology and Equipment, Ministry of Education, Chang'an University, Xi'an, 710064, China

²School of Mechanical Engineering, Northwestern Polytechnical University, Xi'an, 710072, China

E-mail: ¹herbal.he@gmail.com, ²changlehao@gmail.com

ABSTRACT

The free vibration characteristics of a dual split torque transmission are studied in this work. A transverse-torsional coupling dynamic model is developed using lumped parameter method. The natural frequencies and mode shapes are calculated by solving the eigenvalue problem of the differential equations of motion. The vibration modes of the system are classified into translational mode and rotational mode, and the characteristics of the two modes are described in details. The modal strain energy and kinetic energy are introduced to study the impact of mesh stiffness, component masses and moments of inertia. The influence of the concerned parameter on a certain mode can be effectively determined by inspection of the modal energy distribution. The effect of the torsional stiffness of the shaft connecting two stages is also studied. The results presented in this work can provide references for the design of dynamic performance of the split torque transmission.

Keywords: *Split Torque Transmission, Modal Analysis, Mesh Stiffness, Modal Strain Energy, Kinetic Energy*

1. INTRODUCTION

The split torque transmission, also known as power split transmission or split path transmission, has been used in helicopter transmission since 1980s[1, 2]. It integrates the advantages of planet gear train and conventional parallel shaft gear trains. The system is symmetric in the overall, and for each path it is similar with the common gearing. The gears of each branch only transmit a part of the total torque compared to the simple parallel shaft gearing which must transmit the total torque. Therefore the trains have greater stiffness, better impact resistance and increased reliability than the parallel shaft gear train. This kind of transmission is also widely used in marine transmission to meet the demand of large load capacity and low noise.

Several scholars have performed much research to investigate the vibration and dynamic characteristics of the dual split torque transmission. M. Rashidi[3] built a linear dynamic model to search the effects of shaft location and mesh stiffness on the gear mesh forces of two power paths. T.L. Krantz[4] studied the effects of shaft angle, mesh phasing and compound shaft stiffness on the natural frequencies and dynamic response of the system. M. Rashidi and T.L. Krantz[5-7] had

also done a lot of research on the load sharing of the split torque transmission. A.V. Wolff[8] gained the bearing loads and load sharing characteristics for the system which had employed sliding bearings. Z. Yang[9] built a nonlinear torsional dynamic model and performed analysis about the influences of different design parameters.

In the present study, a transverse-torsional coupling dynamic model for a split torque gearbox is proposed. The free vibration characteristics of the system are investigated in the following analysis. Then the formulations to calculate the modal strain energy, support strain energy and kinetic energy for different vibration modes are derived. The effect of the torsional stiffness of connecting shaft is also studied in this paper.

2. DYNAMIC MODELING

The system to be investigated is a dual split torque speed-increasing gear train used in a marine transmission. The schematic diagram of system is shown in Figure 1. The input gear g_1 transfers the input torque to the two double helical gears g_2 and g_3 . Then the gears g_4 and g_5 confluence the torque to the output gear g_6 .

The lumped parameter model of the system is shown in Figure 2. As the symmetry of double helical gears, the axial vibration of all gears is ignored, only the transverse vibration in the horizontal and vertical directions is considered, as well as the vibration in rotation direction. The support and gear mesh are simplified as elastic element, while the gear body and connection are treated as rigid body. The deflections of all gears are described by translational coordinates x_i , y_i , and rotational coordinates u_i ($i=1, \dots, 6$). The rotational coordinates $u_i=r_i\theta_i$, where θ_i is the component rotation; r_i is the base circle radius for each gear. As all the bearings are sliding bearings, the details of bending stiffness are not given in Figure 2, which is only denoted by k_i . According to the dynamic characteristics of oil film in sliding bearings, every k_i includes four items, which are k_{ixx} , k_{ixy} , k_{iyx} , k_{iyy} respectively.

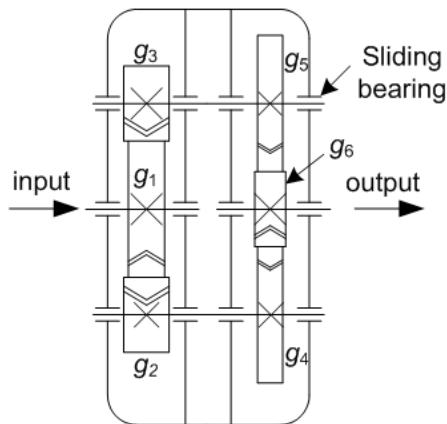


Figure 1: Schematic Diagram Of The System

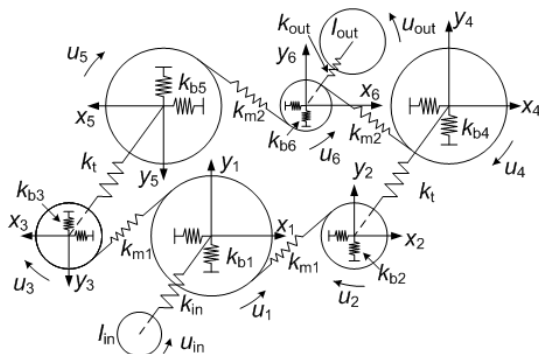


Figure 2: The Dynamic Model Of The System

When neglecting the friction on tooth surfaces, the generalized transverse-torsional coupling dynamic model for a double helical gear pair is illustrated in Figure 3. The subscript 1 is the driver

gear, and the subscript 2 is the driven gear. The relative gear mesh displacement can be denoted as:

$$\delta_{12} = (x_1 \sin \varphi_1 + y_1 \cos \varphi_1 + u_1 - x_2 \sin \alpha - y_2 \cos \alpha - u_2) \cos \beta_b \quad (1)$$

where β_b is the base helix angle, α is the mesh angle, and $\varphi_i = \alpha - \phi_i$, in which ϕ_i is the fixed angle and is 0 and π respectively for the two paths.

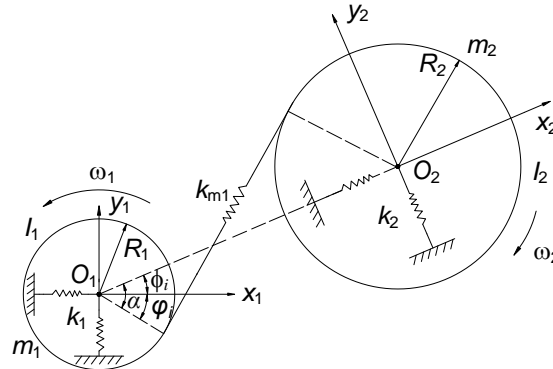


Figure 3: Generalized Model For The Gear Pair

Applying Newton's second law, the undamped differential equations of motion of the input gear g_1 can be derived as:

$$\begin{aligned} m_1 \ddot{x}_1 + k_{1xx} x_1 + k_{1xy} y_1 + \sum_{j=2}^3 k_{m1j} \delta_{1j} \cdot \cos \beta_{b1} \sin \alpha_1 &= 0 \\ m_1 \ddot{y}_1 + k_{1yx} x_1 + k_{1yy} y_1 + \sum_{j=2}^3 k_{m1j} \delta_{1j} \cdot \cos \beta_{b1} \cos \alpha_1 &= 0 \\ m_{eq,1} \ddot{u}_1 + \sum_{j=2}^3 k_{m1j} \delta_{1j} \cdot \cos \beta_{b1} &= \frac{T}{r_1} \end{aligned} \quad (2)$$

where $m_{eq,1} = I_1/r_1$ is the equivalent mass in the rotation direction, I_1 is the moment of inertia of g_1 , T is the input torque. The equations of motion for the other gears can be obtained similarly. Assembling the equations in matrix form as:

$$M \ddot{X} + KX = F \quad (3)$$

where M represents the mass matrix, K is the stiffness matrix, F is exciting force vector, and X is the vector of the degrees of freedom of the system. Without considering the vibration of input shaft and output shaft, the system has a total of eighteen degrees of freedom for the six gears.

3. MODAL ANALYSIS

The parameters of the investigated system are given in Table 1. The natural frequencies and mode shapes can be calculated by solving the associated eigenvalue problem of Equation (3), which is:

$$\lambda_j M \phi_j = K \phi_j \quad (4)$$

where $\lambda_j = \omega_j^2$, ω_j is the j -th natural frequency, ϕ_j is the corresponding mode shape.

Table 1: Parameters Of The System

Gear	g_1	g_2, g_3	g_4, g_5	g_6
Teeth Number	79	44	125	31
Module(mm)	2.25	2.25	1.75	1.75
Face Width(mm)	60	60	40	40
Mass(kg)	36.20	18.31	33.33	4.53
Moment of Inertia (103×kg·mm ²)	139.58	29.4	214.1	1.41
Base Radius(mm)	89.62	49.91	111.6	27.68
Mesh Angle(°)	$\alpha_1=21.53; \alpha_2=21.80$			
Base Helix Angle(°)	$\beta_{b1}=21.27; \beta_{b2}=22.93$			
Mesh Stiffness (kN/μm)	$k_{m1}=1.82; k_{m2}=1.25$			
Bearing Stiffness(kN/μm)	$k_{ixx}=6, k_{ixy}=1, k_{iyx}=0.8, k_{iyv}=4$			
Torsional Stiffness(N·m/rad)	$k_t=1 \times 10^7$			

3.1 Natural Frequencies And Vibration Modes

The natural frequencies of the system are different from each other, and all the mode shapes can be classified into two types: translational mode (TM) and rotational modes (RM). Table 2 outlines the natural frequencies and the corresponding vibration modes. The system is positive semidefinite and therefore has a rigid body mode, with the frequency 0Hz. There are ten translational modes and seven rotational modes for the investigated model.

Table 2: Natural Frequencies And Mode Types

NO.	f (Hz)	Mode type	NO.	f (Hz)	Mode type
1	0	-	10	2449	RM
2	979	TM	11	2487	TM
3	1589	RM	12	3001	RM
4	1655	RM	13	3010	TM
5	1728	TM	14	4000	TM
6	1779	TM	15	4115	RM
7	2163	TM	16	5673	TM
8	2181	RM	17	5855	RM
9	2272	TM	18	7541	TM

The normalized modal deflections for the two vibration modes are shown in Figure 4. For translational modes, the two center gears (g_1, g_6) have pure translational movements, and the rotational deflections are zero. The two branch gears of each stage have opposite deflections in this mode, see Figure 4(a). For rotational modes, the two center gears have pure rotational movements, and the translational deflections are zero. The two branch gears of each stage have identical deflections in this mode, see Figure 4(b).

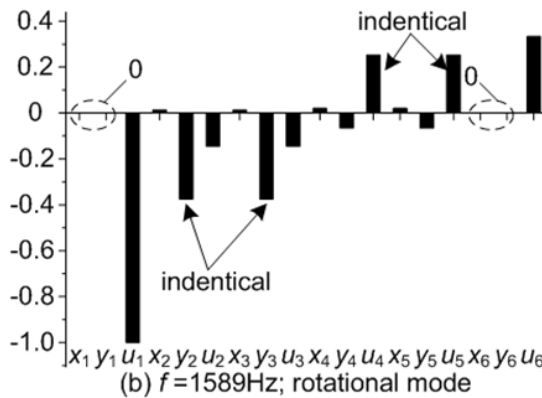
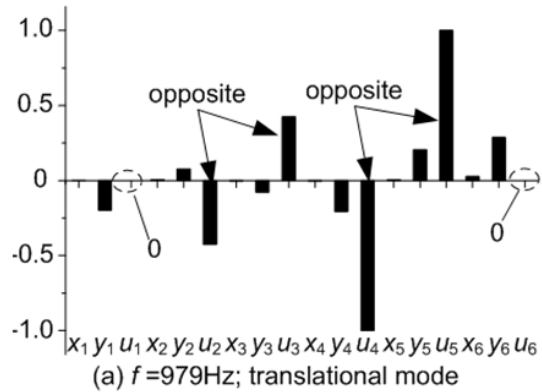


Figure4: The dynamic model of the system

3.2 Sensitivity Of Natural Frequencies To Mesh Stiffness

It was found by J. Lin and R. G. Parker that the natural frequency sensitivity to certain stiffness is uniquely associated with the modal strain energy stored in that spring [10]. The mesh strain energy is generated due to gear distortion, and for the first stage it is defined as:

$$U_{m1} = \sum_{i=2}^3 \frac{1}{2} k_{m1} (\delta_{li})^2 \quad (5)$$

where U_{m1} is the mesh strain energy of first stage, k_{m1} is the mean mesh stiffness, δ_{1j} is the relative deflection as expressed in Equation (1).

The derivative of eigenvalue with respect to mesh stiffness k_{m1} is expressed as:

$$\frac{\partial \lambda_j}{\partial k_{m1}} = \sum_{i=2}^3 (\delta_{1i})^2 = \frac{2U_{m1}}{k_{m1}} \quad (6)$$

Therefore, the mesh strain energy can intuitively reflect the effects of mesh stiffness on the concerned natural frequency. The mesh strain energy of the second stage can be obtained similarly. Figure 5 shows the mesh strain energy for all natural frequencies. As the modal deflection has been normalized, the mesh strain energy calculated here is also dimensionless. The x-axis is the number of every frequency, and y-axis is the relative value of mesh strain energy.

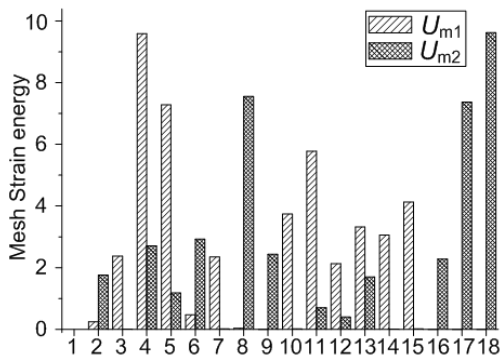


Figure 5: Mesh Strain Energy For All Mode Shapes

It can be obviously seen from Figure 5 that the mesh stiffness of first stage has greater impact on the third, fourth, fifth, seventh, tenth, eleventh, twelfth, thirteenth, fourteenth and fifteenth frequencies than the mesh stiffness of second stage, and the reverse effects are appeared for the other frequencies. The results are consistent with the modal deflections for 979Hz (mode 2) and 1589Hz (mode 3) as depicted in Figure 4. For mode 2, deflections of the second stage is greater than the first stage, so more strain energy is stored in U_{m2} than in U_{m1} . Consequently, ω_2 is more sensitive to k_{m2} than to k_{m1} . In the same way, it can be found that ω_3 is more sensitive to k_{m1} than to k_{m2} .

3.3 Sensitivity Of Natural Frequencies To Bearing Stiffness

Similar to the mesh strain energy, the support strain energies for bearing stiffnesses are defined as:

$$U_i = U_{ixx} + U_{iyx} + U_{ixy} + U_{iyy} = \frac{1}{2} (k_{xx}x_i^2 + k_{yy}y_i^2 + k_{yx}x_i^2 + k_{xy}y_i^2) \quad (7)$$

Where U_i , $i = 1, \dots, 6$ is the total support strain energies in the bearing of gear i , U_{ixx} , U_{iyx} , U_{ixy} , U_{iyy} are the strain energies in the four support springs of sliding bearing, respectively.

The derivative of eigenvalue with respect to bearing stiffness is:

$$\frac{\partial \lambda_j}{\partial k_i} = 2(x_i^2 + y_i^2) = 4 \left(\frac{U_{ixx} + U_{iyx}}{k_{ixx} + k_{iyx}} + \frac{U_{ixy} + U_{iyy}}{k_{ixy} + k_{iyy}} \right) \quad (8)$$

Figure 6 shows the distribution of strain energies for all bearings in 979Hz and 1589Hz. As the description in Figure 4, the branch gears have the opposite or the identical modal deflections for the two mode types, so the strain energies of the branch gears are equal. The natural frequency ω_2 (979Hz) is most sensitive to the bearing stiffness of g_6 , and ω_3 (1589Hz) is most sensitive to the bearing stiffness of g_2, g_3 . It can be also seen that the rotational mode (1589Hz) is independent of the bearing stiffness of the center gears g_1 and g_6 because there are no modal deflections for them in this mode.

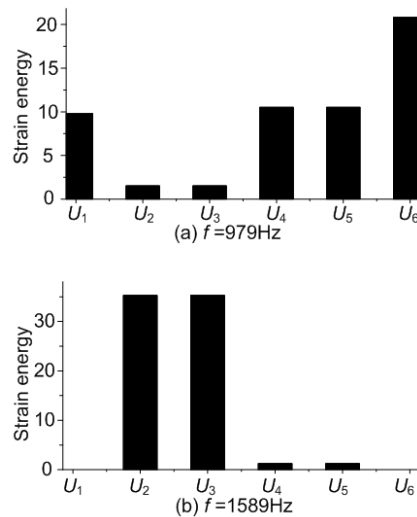


Figure 6: Support strain energy of all bearings

3.4 Sensitivity Of Natural Frequencies To Mass Property

The modal kinetic energy of the system is defined as:

$$T_i = \frac{1}{2} \omega_j^2 m_i (x_i^2 + y_i^2) \quad (9)$$

$$T_{i,u} = \frac{1}{2} \omega_j^2 m_{eq,i} u_i^2 \quad (10)$$

where T_i ($i=1,2,\dots,6$) is the translational kinetic energy of different gears, $T_{i,u}$ ($i=1,2,\dots,6$) is the kinetic energy associated with a certain moment of inertia.

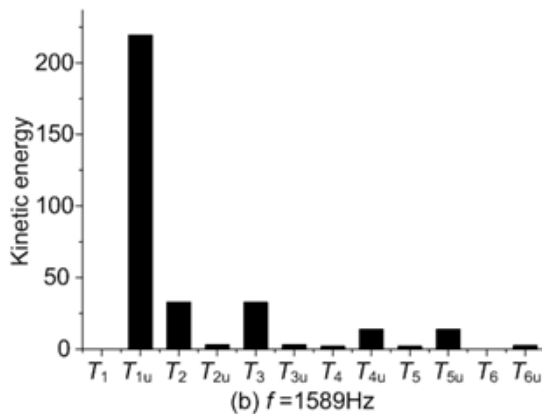
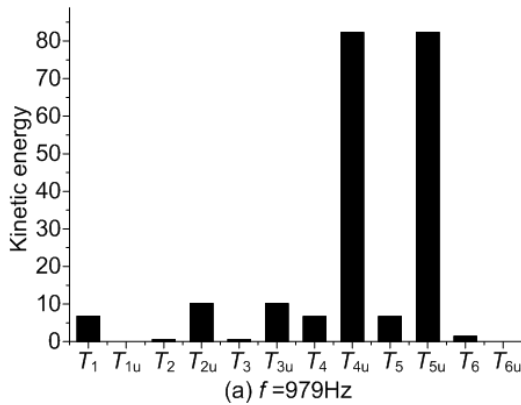


Figure 7: Distribution Of Kinetic Energies

The derivative of eigenvalue with respect to mass is expressed as:

$$\frac{\partial \lambda_j}{\partial m_i} = -\lambda_j (x_i^2 + y_i^2) = -\frac{2T_i}{m_i} \quad (11)$$

$$\frac{\partial \lambda_j}{\partial m_{eq,i}} = -\lambda_j u_i^2 = -\frac{2T_{i,u}}{m_{eq,i}} \quad (12)$$

Therefore, the kinetic energies can be used to estimate the impact of mass properties on different frequencies. Figure 7 shows the distribution of kinetic energies in 979Hz and 1589Hz. As can be seen in Figure 7(a), the moments of inertia of g_4, g_5 have significant effect on the natural frequency 979Hz. We can conclude that the rotational deflections of g_4 and g_5 may be the principal deflections in 979Hz. After observing the mode

shapes of 979Hz, the conclusion agrees well with the description in Figure 4(a). The masses of g_1, g_4, g_5 and the moments of inertia of g_2, g_3 have comparatively small effect; while the others have little effect on the mode shape in 979Hz. Besides, for T_{1u} and T_{6u} are equal to zero, the mode shape in 979Hz is independent of the inertias of the center gears. Figure 7(b) indicates that the moment of inertia of g_1 is the main factor that affects the mode shape of 1589Hz, and the masses of center gears have no effects on this mode shape.

3.5 Effect of Connecting Shaft

The natural frequencies are calculated as the torsional stiffness of connecting shaft k_t is varied from 1×10^7 N/m to 3×10^7 N/m. It can be seen from Figure 8 that with the variation of shaft stiffness, most of the natural frequencies do not change except mode 14 and mode 15. The natural frequencies of mode 14 and mode 15 will increase linearly with the increase of shaft stiffness. It's observed from Figure 9 that the modal deflections of g_2 and g_3 are the major components of the mode shapes for mode 14 and mode 15. Therefore, the shaft stiffness mainly affects the vibration of adjacent pinions but not the large gear.

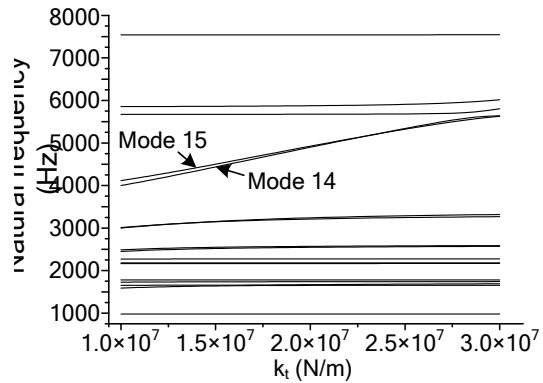


Figure 8: Natural Frequencies Versus The Shaft Stiffness

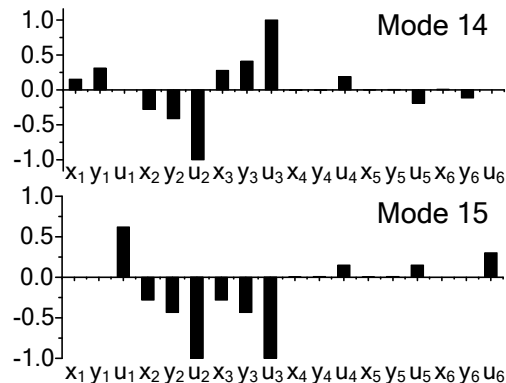


Figure 9: Mode Shapes When K_t Equals To 1×10^7 N/M

4. CONCLUSION

A dynamic model of a split torque transmission has been developed in order to investigate the free vibration characteristics of the system. The influence of several key design parameters have been studied in this paper. There are two vibration modes for the split torque transmission: translational mode and rotational mode. The simplified formulae for mesh strain energy, support strain energy can directly reflect the influences of mesh stiffness and bearing stiffness on a certain vibration mode. The bearing stiffness has no effect on the center gears in rotational mode. The mode shape in rotational mode is independent of the masses of the center gears, while the translational mode is independent of the moments of inertias of the center gears. The variation of the torsional stiffness of the connecting shaft mainly has impact on its adjacent pinions and the corresponding natural frequencies. Future work will aim at the dynamic response and load sharing analysis of the split torque system.

ACKNOWLEDGEMENT

This work is supported by the National Natural Science Foundation of China (51205029) and the Special Fund for Basic Scientific Research of Central Colleges, Chang'an University (CHD2011JC177).

REFERENCES:

- [1] G. White, "Split-Torque Helicopter Transmission with Widely Separated Engines", *Proceedings of the Institution of Mechanical Engineers, Part G: Journal Aerospace Engineering*, Vol. 203, No.G1, 1989, pp.53-65.
- [2] Jules G. Kish, "Sikorsky Aircraft Advanced Rotorcraft Transmission", *NASA Contractor Report 191079*, 1993.
- [3] M. Rashidi, T. L. Krantz, "Dynamics of a Split Torque Helicopter Transmission", *NASA Technical Memorandum 105681*, 1992.
- [4] T. L. Krantz, M. Rashidi, "Vibration Analysis of a Split Path Gearbox", *NASA Technical Memorandum 106875*, 1996.
- [5] T. L. Kranz, M. Rashidi and J.G.. Kish, "Split Torque Transmission Load Sharing", *NASA Technical Memorandum 105884*, 1992.
- [6] T. L. Krantz, "A Method to Analyze and Optimize the Load Sharing of Split Path Transmissions", *NASA Technical Memorandum 107201*, 1996.
- [7] T. L. Krantz, I. R. Delgado, "Experimental Study of Split-Path Transmission Load Sharing", *NASA Technical Memorandum 107202*, 1996.
- [8] A. V. Wolff, "Analysis of a Split-Path Gear Train with Fluid-Film Bearings", *Virginia Polytechnic Institute and State University*, Master Thesis, 2004.
- [9] Z. Yang, S. M. Wang and Y.S. Fan, "Nonlinear Dynamics Characteristics of Split-torque Gear Transmission System", *Chinese Journal of Mechanical Engineering*, Vol.44, No.7, 2008, pp.52-57.
- [10] J. Lin, R. G. Parker, "Sensitivity of Planetary Gear Natural Frequencies and Vibration Modes to Model Parameters", *Journal of Sound and Vibration*, Vol.228, No.1, 1999, pp.109-128.